Measurement 218 (2023) 113258

Contents lists available at ScienceDirect

Measurement

journal homepage: www.elsevier.com/locate/measurement

Single body sensor for calibration of Spring-Mass-Damper parameters in biodynamic pedestrian modelling

Chiara Bedon

University of Trieste, Department of Engineering and Architecture, Piazzale Europa 1, 34127 Trieste, Italy

ARTICLE INFO

Keywords:
Human-Structure Interaction (HSI)
Human-induced effects
Pedestrian structures
Spring-Mass-Damper (SMD) models
Body Centre of Mass (CoM)
Experiments
Numerical analyses
Structural performance indicators

ABSTRACT

For structural design and vibration monitoring purposes, several simplified equivalent-force models or more complex computational strategies are available to describe Human-Structure Interaction (HSI) phenomena on pedestrian systems, and in particular the vertical reaction forces induced by walking occupants. Among others, various Spring-Mass-Damper (SMD), Single Degree of Freedom (SDOF) biodynamic models of literature can be used to mechanically describe a single pedestrian in the form of equivalent body mass m, spring stiffness k and viscous damping coefficient c. Basically, existing SMD formulations are characterized by specific theoretical assumptions and (often complex) experimental methods for the calibration of m, k, c. Usually, SMD parameters can be optimally quantified when multiple sensors (on pedestrian's body and on the structure) are used to capture motion features and the corresponding reaction force. In this paper, body accelerations of a pedestrian are tracked by means of a single Centre of Mass (CoM) sensor and are elaborated to derive basic input parameters for an alternative, newly optimized SMD model. Experimental registrations from a total of 30 random walks and more than 300 gaits (on rigid floor) are taken into account, and fitting expressions for m, k, c are proposed. The present SMD formulation (SMD-0) is validated towards a selection of literature proposals (SMD-1 to SMD-4), based on parametric numerical dynamic analyses (100 in total), which are carried out by taking into account various pacing frequencies (f_p = 1.5–2 Hz the explored range) and four different pedestrian structures / floors (F#1 to F#4). The comparison of classical performance indicators for human-induced structural vibrations proves the efficiency and potential of current SMD-0 approach, and suggests further investigations in support of optimized protocols.

1. Introduction

For structural systems characterized by low vibration frequency and high slenderness (i.e., like bridges or floors), the analysis of Human-Structure Interaction (HSI) phenomena and the quantitative measure of their effects (especially the vertical reaction force) are crucial steps for vibration serviceability assessment [1,2], and generally requires dedicated calculation methodologies. Among others [3], efficient biodynamic pedestrian models take often the form of Spring-Mass-Damper (SMD), Single Degree of Freedom (SDOF) systems, which – above appropriate calibration – can capture body motion features and human-induced effects of single pedestrians on rigid or flexible structures (Fig. 1).

In this regard, several robust analytical proposals can be found in literature (see for example [4–8] and others), where SMD parameters are calibrated with the support of experimental investigations and numerical validations. The use of SMD models is especially recommended for "low-frequency" structural systems (i.e., with fundamental structural frequency $f_1 < 8$ Hz [2]), due to their relatively high sensitivity to vibrations [1].

In practical terms, the intrinsic advantage of biodynamic SMD models consists in the mechanical description of pedestrians as simple SDOFs, that is in terms of equivalent mass m, stiffness k and viscous damping coefficient c. Overall, the dynamic problem in Fig. 1 involves in fact the mechanical interaction of a walking SMD pedestrian (with own frequency f_m) and a supporting structure / floor characterized by mass M_s, fundamental vibration frequency f_1, damping ratio ξ_s, and (under certain conditions) possible sensitivity to human-induced vibrations.

Usually, multiple sensors are required to track the pedestrian motion and the human-induced effects on floors [4–8], and thus to experimentally support the analytical calibration of m, k, c parameters. In this paper, the attention is given to the assessment and validation of a computationally efficient SMD calibration strategy, where the number of sensors for the experimental analysis is minimized to the unit. A major

E-mail address: chiara.bedon@dia.units.it.

https://doi.org/10.1016/j.measurement.2023.113258
Received 1 January 2023; Received in revised form 13 June 2023; Accepted 26 June 2023
Available online 30 June 2023

advantage is in fact taken from experimental body CoM accelerations recorded for a single pedestrian, for a total of 30 random walks (with up to 300 gaits) on a rigid floor (i.e., concrete laboratory foundation system [9,10]). Input SMD features are calibrated from the elaboration of collected CoM acceleration time histories, and empirical expressions are presented to estimate the spring stiffness k and the damping coefficient c, of the moving pedestrian (with equivalent mass m set equal to real mass M), in the pacing frequency range $f_p = 1.2 \div 2$ Hz.

For the validation of present calibration proposal ("SMD-0", in the following), four existing SMD approaches of literature are taken into account ("SMD-1" to "SMD-4"). A parametric dynamic numerical investigation is carried out (with 100 simulations in total) by taking into account four different floors (F#1 to F#4), to assess and quantitatively compare human-induced effects in the form of typical structural performance indicators. In doing so, see Section 5, normal walking configurations for a single pedestrian are explored in the range $f_p = 1.5 \div 2$ Hz, showing a rather good agreement and potential of present SMD-0 strategy.

2. Spring-Mass-Damper (SMD) biodynamic pedestrian modelling

2.1. Existing approaches

The increasing number of structural applications involving pedestrian systems with high sensitivity to human traffic and human-induced vibrations confirms that refined calculation methods and dedicated studies thus required for many constructed facilities. Typical examples take the form of footbridges with high flexibility and / or long span [11–13], floor systems based on the use of innovative materials [14,15], or even existing pedestrian systems suffering for specific sensitivity to dynamic performances and ambient influencing parameters [16,17].

In this regard, SMD models are particularly advantageous for vibration serviceability assessment purposes, because they are rather accurate to describe real and generally complex pedestrian behaviours (i.e., Fig. 2 [18]), and at the same time they allow to minimize the average cost of simulations.

The basic SMD assumption, see Fig. 3, is that Centre of Mass (CoM) of pedestrian is used to lump the equivalent body mass m. The moving pedestrian is thus mechanically described in the form of SDOF model with spring stiffness k and damping coefficient c. The calibration of m, k, c parameters, according to literature, represents a critical task, because sensitive to a multitude of possible influencing parameters. As such, several proposals and formulations can be found in the literature for an efficient SMD biodynamic model characterization (see for example Section 2.3).

The simplest calculation approach, as known, is represented by equivalent time-varying deterministic forces [2], or even moving deterministic forces [11], for the description of vertical reactions due to pedestrians. Whilst of simple application, equivalent-force procedures have major intrinsic limitations in the representation of reactions by means of Fourier series. Such a modelling assumption is in fact particularly efficient in computational terms, but fully disregards the dynamic interaction between pedestrian and the supporting structure (i.e., HSI phenomena). In this sense, deterministic force methods are accurate for structural systems in which HSI phenomena are less relevant. On the other side, increasingly complex bipedal and even three-dimensional biodynamic models can be used for highly sophisticated HSI calculation purposes and vibration serviceability assessment of pedestrian structures, see for example [19–22].

2.2. Present calibration strategy

Over the years, several experimental and theoretical studies have been elaborated in literature to efficiently calibrate the input SMD biodynamic features (m, k, c) for the analysis of pedestrians on slender and flexible structures (Figs. 1 and 2).

Most importantly, according to literature, the experimental calibration of key parameters for mechanical models like in in Fig. 1 (a) should cover a relatively wide set of pedestrians (i.e., gender, age, height, mass, etc.), floors (i.e., M_s, f_1, etc.), walking configurations (i.e., slow, normal, fast) and pacing frequencies f_p. This kind of SMD calibration usually necessitates of multiple sensors (on body pedestrian and on floor), to track body motion features (on the pedestrian side) and corresponding human-induced reaction forces (on the structural side), and thus to extrapolate efficient empirical expressions for m, k, c.

In this paper, the attention is given to SDOF calibration based on the elaboration of a minimum of experimental measurements from single sensor on pedestrian body. Differing from literature formulations (i.e., Section 2.3), SMD biodynamic parameters are in fact calibrated from body CoM motion features, which are implicitly used, during the experiments, to track human-induced vertical reaction forces on the structure. Such a calibration approach is in line with inverted pendulum assumptions (i.e., Fig. 3) and tries to maximize relevant outcomes for SMD characterization, based on minimization of number of sensors / experimental configurations.

In this sense, the current SMD-0 proposal could be particularly useful when the available resources and instruments for experimental investigations are not sufficient [9,10], or in case of rapid / expeditive experimental diagnostics required for in-service structures [10,23,24], with practical difficulties compared to laboratory experiments.

As a basic condition, the SMD-0 approach is based on the assumption that, for a pedestrian with real mass M, the vertical induced force $F_z(t)$, in time t, is proportional to CoM acceleration $a_z(t)$ and can be estimated from Newton's second law of motion, that is:

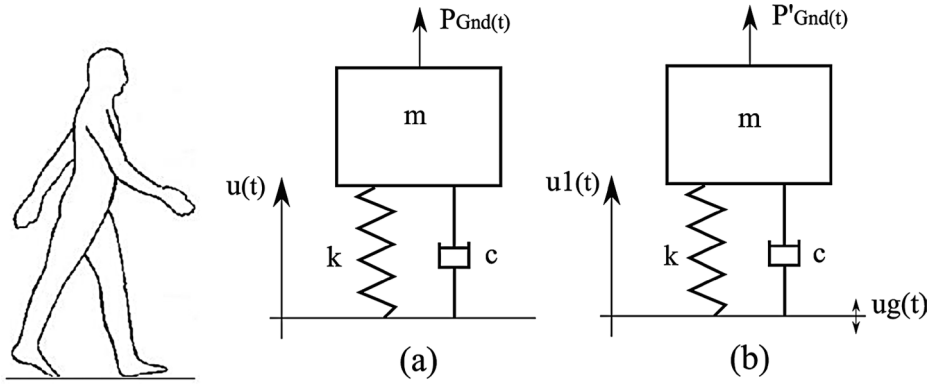

Fig. 1. Biodynamic pedestrian model: schematic mechanical system for a walking human on (a) rigid or (b) flexible structure (reproduced from [6] with permission from Elsevier©, license number agreement 5458710774818, December 2022).

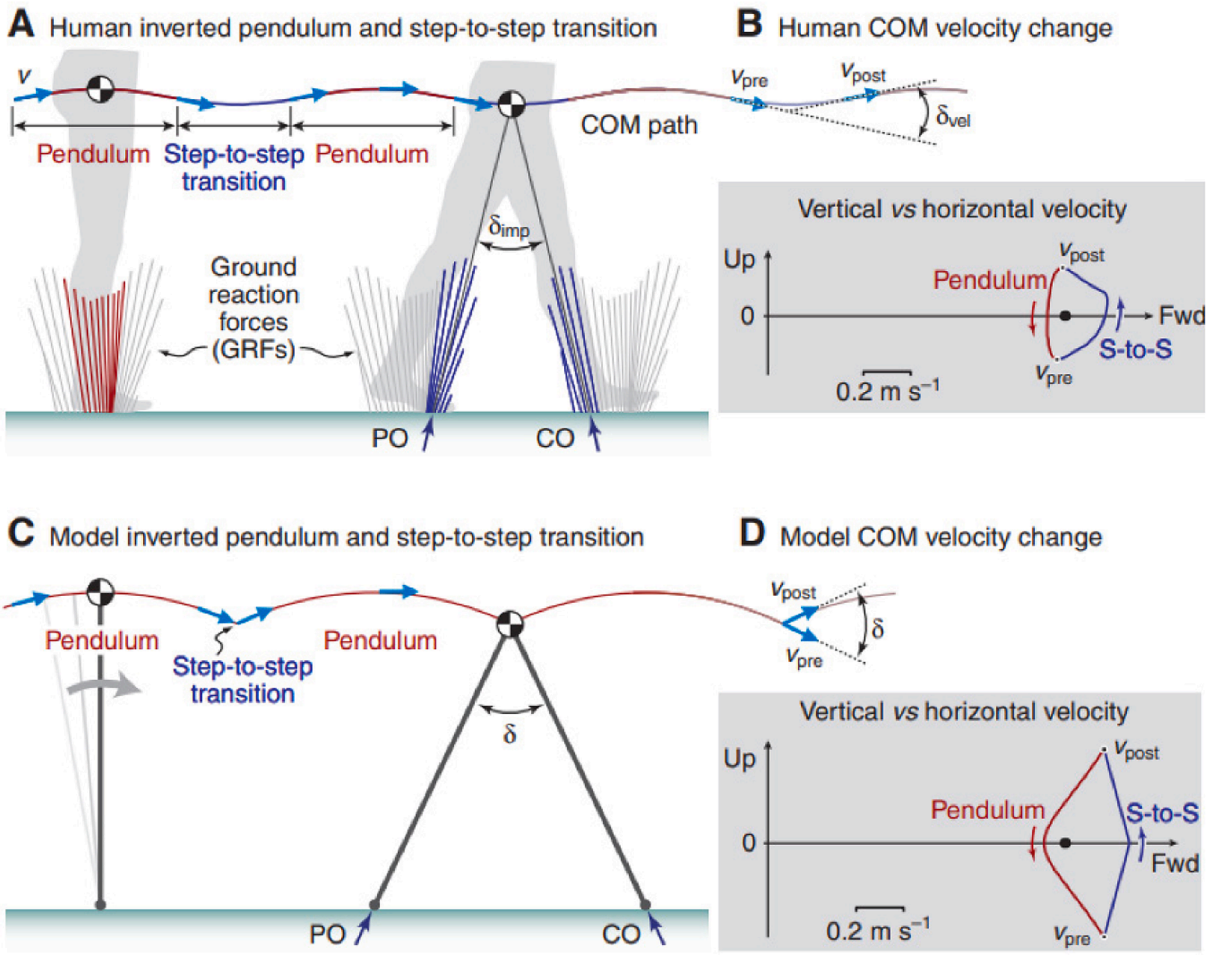

Fig. 2. Schematic representation of inverted pendulum model for a walking pedestrian, with evidence of CoM path and vertical trajectory during motion (figure reproduced from [18] with permission from The Company of Biologists®, copyright license agreement n. 1175262, December 2022).

$$F_Z(t) = Ma_Z(t) \quad (1)$$

At the same time, however, $F_z(t)$ is also proportional to SDOF stiffness k (which is representative of pedestrian's legs), as well as to the vertical motion path of body CoM, $\triangle h(t)$, which further depends on the typical CoM trajectory schematized in Fig. 3 [18], and can be also affected by floor flexibility:

$$F_Z(t) = k \bullet \Delta h(t) \quad (2)$$

By equalling Eqs. (1) and (2), given that body features are known and CoM acceleration in Eq. (1) is tracked, basic SMD properties (m, k, c) can be efficiently calculated. The present experimental setup assumes that the lower is floor rigidity, the lower is the measured leg stiffness, and thus the corresponding CoM acceleration and CoM vertical trajectory

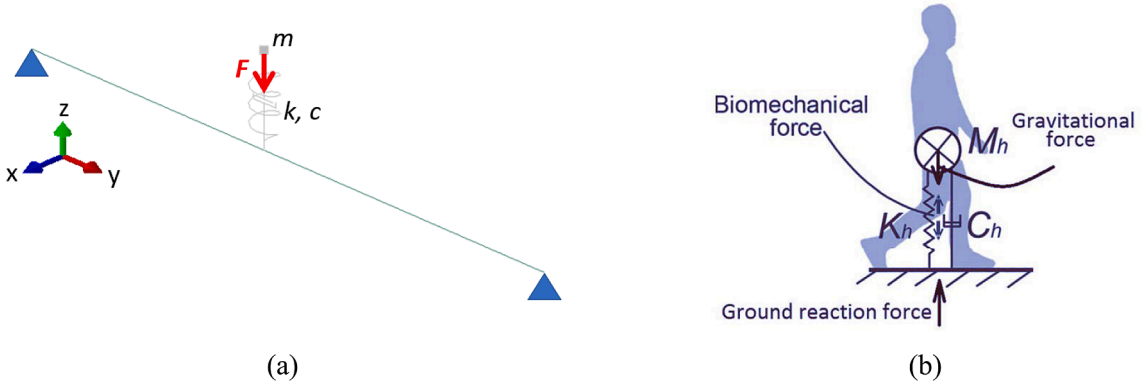

Fig. 3. Biodynamic pedestrian modelling: (a) example of structural model for HSI analysis and (b) schematic representation of Spring-Mass-Damper (SMD), Single Degree of Freedom (SDOF) model (figure reproduced from [8] with permission from Elsevier©, license number agreement 5458701302374, December 2022).

modification.

More precisely, assuming that $m = M$ for SMD-0 model, the undamped and damped pedestrian frequencies are given respectively by:

$$f_m = \sqrt{\frac{k}{m}} \bullet \frac{1}{2\pi} \tag{3}$$

and

$$f_{md} = f_m \bullet \sqrt{1-\xi^2} \tag{4}$$

The estimation of damping ratio ξ and corresponding viscous damping coefficient c can be obtained from iterative calculations in terms of undamped and damped frequencies as in Eqs. (3) and (4), considering that:

$$\xi = \frac{c}{2m\omega_m} \tag{5}$$

and

$$\omega_{md} = \omega_m - \sqrt{1-2\xi^2} \tag{6}$$

where ω_m and ω_{md} represent the associated undamped and damped pulsations.

The iteration in Eqs. (3) to (6) is repeated in terms of viscous damping coefficient c, until the estimated frequency converges. To note that the assumption in Eq. (6) is in line with some past SMD literature elaborations, see for example [4].

The novelty of present proposal is represented by use of single CoM sensor to account for body motion features, and their progressive modification on different structures. As far as the floor is more rigid or flexible, HSI phenomena change and thus the input of Eq. (2) also varies, because both leg stiffness and CoM trajectory implicitly change, in the same way of the measured acceleration in Eq. (1).

Following the above assumptions, experimental investigations are discussed in Section 3 and empirical expressions are formulated for the estimation of SMD parameters. Successively, parametric numerical analyses are arranged in Section 4 and presented in Section 5, for validation of present SMD-0 formulation towards the selection of literature approaches as in Section 2.3.

Most importantly, it has to be noted that random walks were carried out and tracked, in present study, by the same individual pedestrian over a rigid concrete, laboratory foundation system. In this sense, a major intrinsic limitation could be represented by lack of multiple pedestrians, for sensitivity analysis of SMD parameters and structural performances to various SMD strategies. Also, the supporting records were measured on a rigid substrate [9], rather than on different floor configurations. In this regard, it was experimentally proved in [10], with the same experimental setup as in Fig. 4, that human-induced reaction forces and the corresponding dynamic load factors can be efficiently extrapolated. Moreover, for pedestrians moving on flexible floors, human-induced effects (and thus SMD parameters) are typically lower than on rigid structures. The present SMD-0 elaboration and outcomes, in this regard, extend the experimental evidences from [10] and take advantage from previous confirmations to use them for a possibly efficient biodynamic calibration.

2.3. Selected literature SMD models

Among others, the SMD calibration strategies reported in [5–8] were taken into account for quantitative analysis of structural performances.

Silva et al. [5], SMD-1 in the following, elaborated a regression model for SMD biodynamic parameters in which m, c and k can be calculated as a function of pacing frequency f_p and real pedestrian mass M. More precisely, m is defined as a function of f_p and M, while c is fitted to m, and k derives from c:

$$m = m(f_p, M) = 97.082 + 0.275M - 32.52f_p \tag{7}$$

$$c = c(m) = 107.455 + 16.208m \tag{8}$$

$$k = k(c) = 5758.441 + 11.103c \tag{9}$$

A similar proposal can be found [6], SMD-2 model by Toso et al., where the experimental evidences from a total of 35 instrumented pedestrians were further elaborated by Artificial Neural Network, to correlate their biodynamic parameters as a function of a basic walking feature (namely, the pacing frequency f_p). The final proposal resulted in:

$$m = m(f_p, M) = -231.34 + 3.69M + 154.06f_p - 1.97Mf_p + 0.005M^2 - 15.25f_p^2 \tag{10}$$

$$c = c(M, m) = -1115.69 + 92.56M - 108.94m + 2.91Mm - 1.33M^2 - 1.30m^2 \tag{11}$$

$$k = k(M, f_p) = 75601.45 - 1295.32M - 33786.75f_p + 506.44Mf_p + 3.59M^2 + 539.39f_p^2 \tag{12}$$

The calibration approach followed by Pfeil et al. [7], noted as SMD-3 model in present study, included a number of experimental measurements for pedestrians walking on both a rigid floor and a flexible laboratory platform (with slow, normal or fast motion). The calibration proposed in [7] assumes a reduction in equivalent mass m for pedestrian, and a spring stiffness k which is linearly proportional to m:

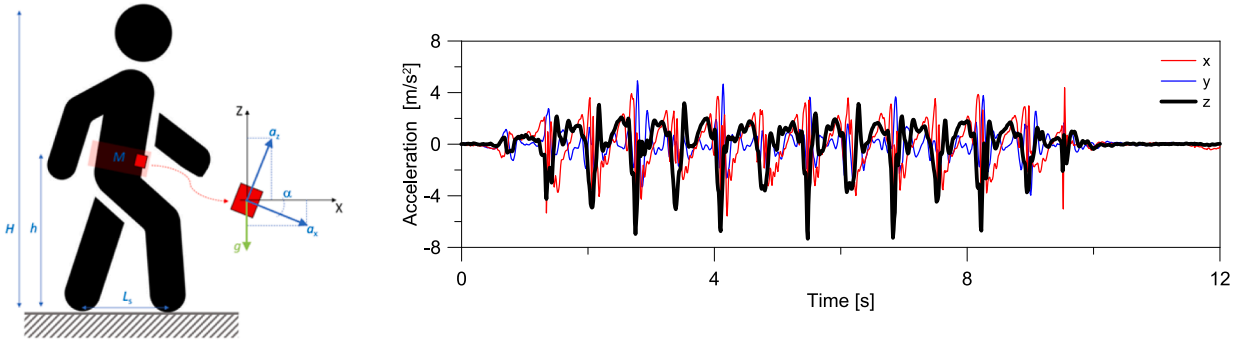

(a) (b)

Fig. 4. Experimental setup and measurements for the present SMD model calibration (SMD-0): (a) single sensor in body CoM of pedestrian; (b) example of acceleration components during normal walks (figures reproduced from [9] under the terms and conditions of CC-BY license agreement).

$$m = m(f_p, M) = 0.874M - 9.142f_p + 12.94 \quad (13)$$

$$k = k(m) = 360.3m - 1282.5 \quad (14)$$

To note that the damping coefficient c, based on [7], must be estimated from iterative calculations in terms of damping ratio ξ, as a function of the damped frequency f_{md} of pedestrian model, that is:

$$\xi = \xi(f_{md}) = -20.818f_{md} + 87.513 \quad (15)$$

with f_m and f_{md} given by Eqs. (3) and (4).

The iterative calculation based on Eqs. (15) and (3)-(4) ends when ξ converges.

Finally, the calibration proposal by Wang et al. [8], SMD-4 model, assumes that $m = M$ and:

$$f_m = f_m(f_p) = 0.3049f_p + 1.367 \quad (16)$$

with the damping coefficient depending on the pacing frequency:

$$c = c(f_p) = -0.2116f_p + 0.8737 \quad (17)$$

and thus the spring stiffness k can be extracted from Eq. (3).

3. Present proposal (SMD-0)

3.1. Experimental setup and calibration strategy

In this paper, a total of 30 walking records (with up to 300 gaits) like in Fig. 4 were taken into account and elaborated according to Eqs. (1) to (6), in order to extract (assuming $m = M$) the spring stiffness k and damping coefficient c of an individual pedestrian.

To note that a single adult volunteer (female, 39 years, 1.85 m high, with $m = M = 80$ kg) was involved in the investigation. An acquisition system consisting of a wi-fi micro electro-mechanical system (MEMS), triaxial sensor fixed on body CoM was used during the experimental investigation [9], see Fig. 4 (a). The sensor in use, see also [9,10] was chosen to track the acceleration and inclination components of body CoM in time, and thus to extract relevant input records for Eqs. (1) and (2).

By equalling Eqs. (1) and (2), basic SMD properties of pedestrian can in fact be extracted by assuming that $m = M$ is known for the involved volunteer, in the same way of total height H and CoM height h in Fig. 4 (a). The vertical acceleration component, $a_Z(t)$, can in fact be efficiently extracted from single CoM triaxial sensor, given that [9]:

$$a_Z(t) = a_z(t)cos\alpha(t) - a_x(t)sin\alpha(t) \quad (18)$$

The experimental setup in Fig. 4 has a key role in the extraction of SMD parameters (with $m = M$), and in particular the SMD stiffness k and successively the damping coefficient c.

More precisely:

- From a typical experimental record of acceleration time history as in Fig. 4 (b), where a specific pacing frequency f_p is imposed to the walking volunteer, the vertical reaction $F_z(t)$ in Eq. (1) can be first efficiently calculated.
- The required input for Eq. (2) also derives from the CoM acceleration records as in Fig. 4. It is fact known that the vertical path $\triangle h(t)$ of CoM trajectory during walks corresponds to the double integration of vertical acceleration $a_Z(t)$ in time (from Eq. (17)). As such, the SMD spring stiffness k can be directly extrapolated from combination of Eqs. (1) and (2).
- Once k is known, c is obtained from iterative calculations in Eqs. (3) to (6), and the same approach can be repeated to cover a sufficient number of pacing frequencies f_p.

3.2. Practical steps for derivation of input parameters

The present study took advantage from a set of 30 body CoM acceleration records reported in [9]. To this aim, it is important to remind that each walk record was characterized by a minimum number of 10 gaits, for a total of 300 records. The calibration of spring stiffness k was first carried out – based on Eqs. (1) and (2) – for single gait records of each recorded walk. A typical example is shown in Fig. 5, where k is reported for each gait (10 in total) of a single walk setup, as a function of f_p.

The average k value for each walk (30 in total) was then taken into account, as a function of average f_p, for the final SMD calibration. In this regard, major elaborations and signal processing analyses were carried out with the support of a Matlab® toolbox [25].

3.3. Empirical expressions for SMD-0

Fig. 6 shows, in average values for 300 gaits, the typical results of calculation outcomes carried out, in terms of k and c, in accordance with the flowchart of Fig. 5.

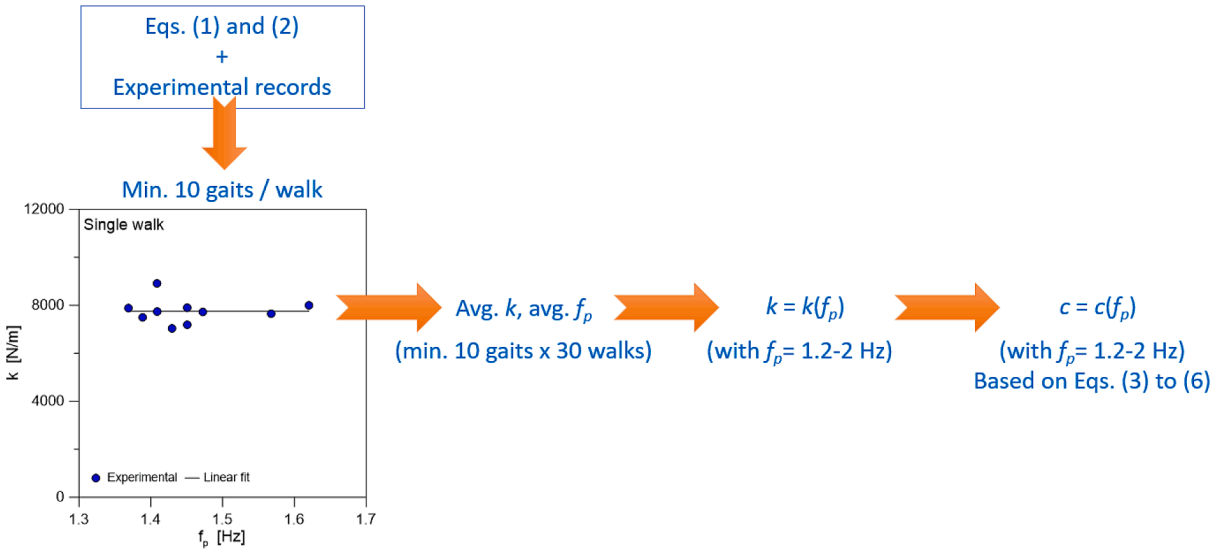

Fig. 5. Flowchart for present experimental derivation of spring stiffness k and damping coefficient c for the proposed SMD-0 modelling strategy.

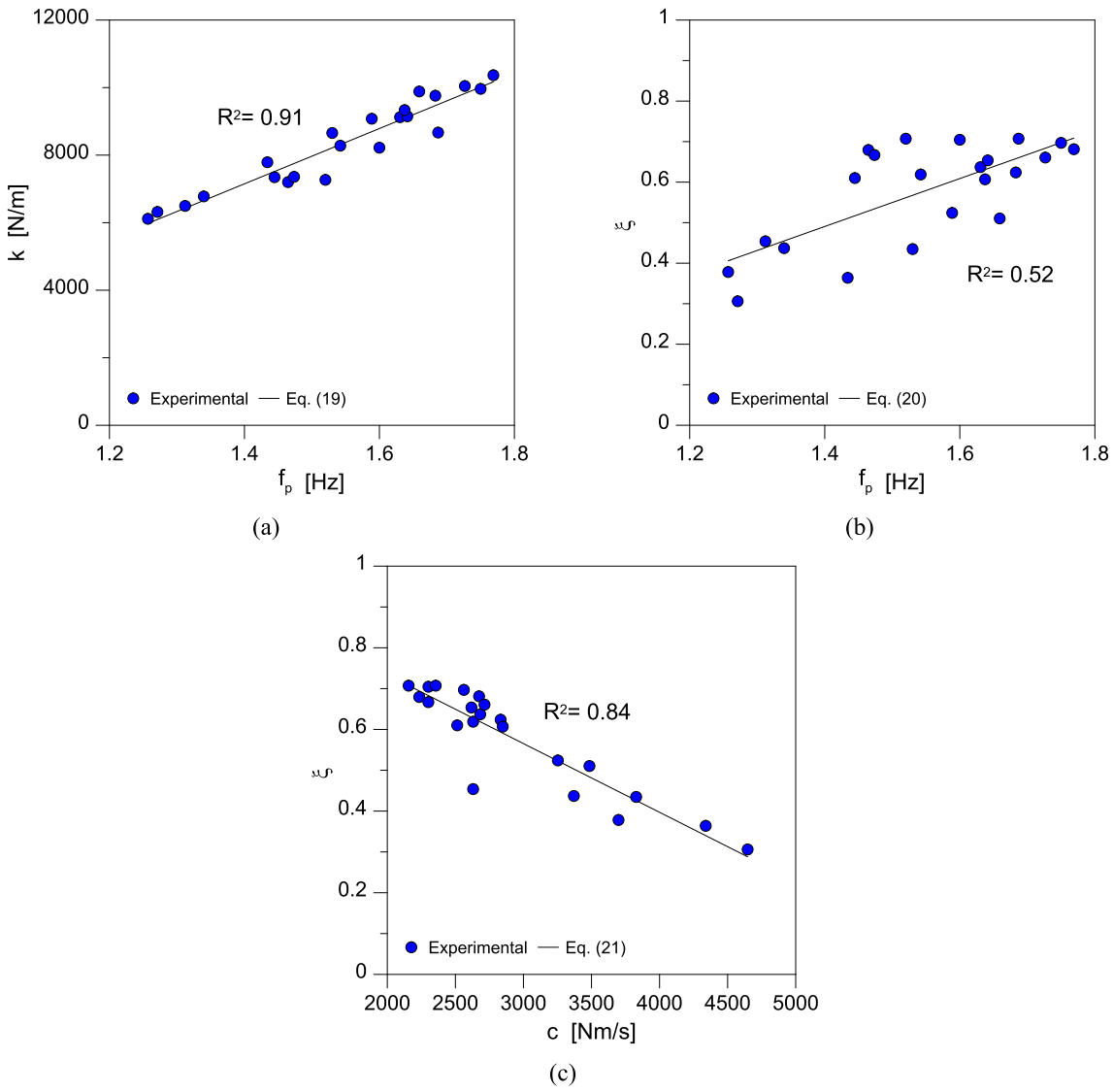

Fig. 6. Experimental derivation of presently proposed biodynamic model parameters (SMD-0), as a function of pacing frequency f_p: (a) spring stiffness k; (b) damping ratio ξ, with (c) damping ratio-coefficient trends.

As shown in Fig. 6 (a), the spring stiffness k linearly increases with pacing frequency f_p (with $R^2 = 0.91$ the calculated coefficient of correlation), and this trend is in line with several literature studies. In terms of damping ratio ξ, which is directly involved in Eqs. (3) to (6), the typical trend is shown in Fig. 6 (b). For present investigation, a linear fit was assumed for simplicity ($R^2 = 0.52$), in a range spanning from 0.3 to 0.7, for the explored f_p interval. Finally, Fig. 6 (c) shows the correlation of damping ratio and coefficient ($R^2 = 0.84$), as a function of f_p.

From a qualitative and quantitative point of view, it is worth to note that a rather good agreement of present estimates was generally observed with experimental literature studies. The experimentally derived damping ratio ξ reported in [26] for various involved pedestrians, for example, was found to span between 0.4 and 0.7, for walking velocities in the range of 0.8 to 2.2 m/s, and this is in line with Fig. 6 (b). The corresponding spring stiffness k [26] was calculated in a minimum of 2,000 N/m and up to around 13,000 N/m, for a walking speed of 2 m/s, which is also rather in accordance with Fig. 6 (a).

In practical terms, the experimental results in Fig. 6 are particularly useful because they support the definition of empirically expressions for the input SMD-0 parameters, as a function of pacing frequency f_p (in Hz), that is:

$$k = 8190 f_p - 4315.8 \quad (\text{with } R^2 = 0.91) \tag{19}$$

where k is given in N/m,

$$\xi = 0.5915 f_p - 0.3375 \quad (\text{with } R^2 = 0.52) \tag{20}$$

Finally, based on Fig. 6 (c), it is observed that:

$$\xi = 1.0705 - 0.0002c \quad (\text{with } R^2 = 0.84) \tag{21}$$

and present SMD-0 elaborations are extrapolated in the range $f_p = 1.2$–2 Hz.

3.4. Correlation of SMD-0 parameters and literature models

As far as the governing empirical expressions for SMD-0 proposal are achieved, the first issue is to assess the corresponding estimates towards existing literature approaches. Fig. 7, in this regard, gives evidence of presently calibrated SMD-0 model and selected SMD formulations (i.e., Section 2.3), for walking configurations with $f_p = 1.5$–2 Hz.

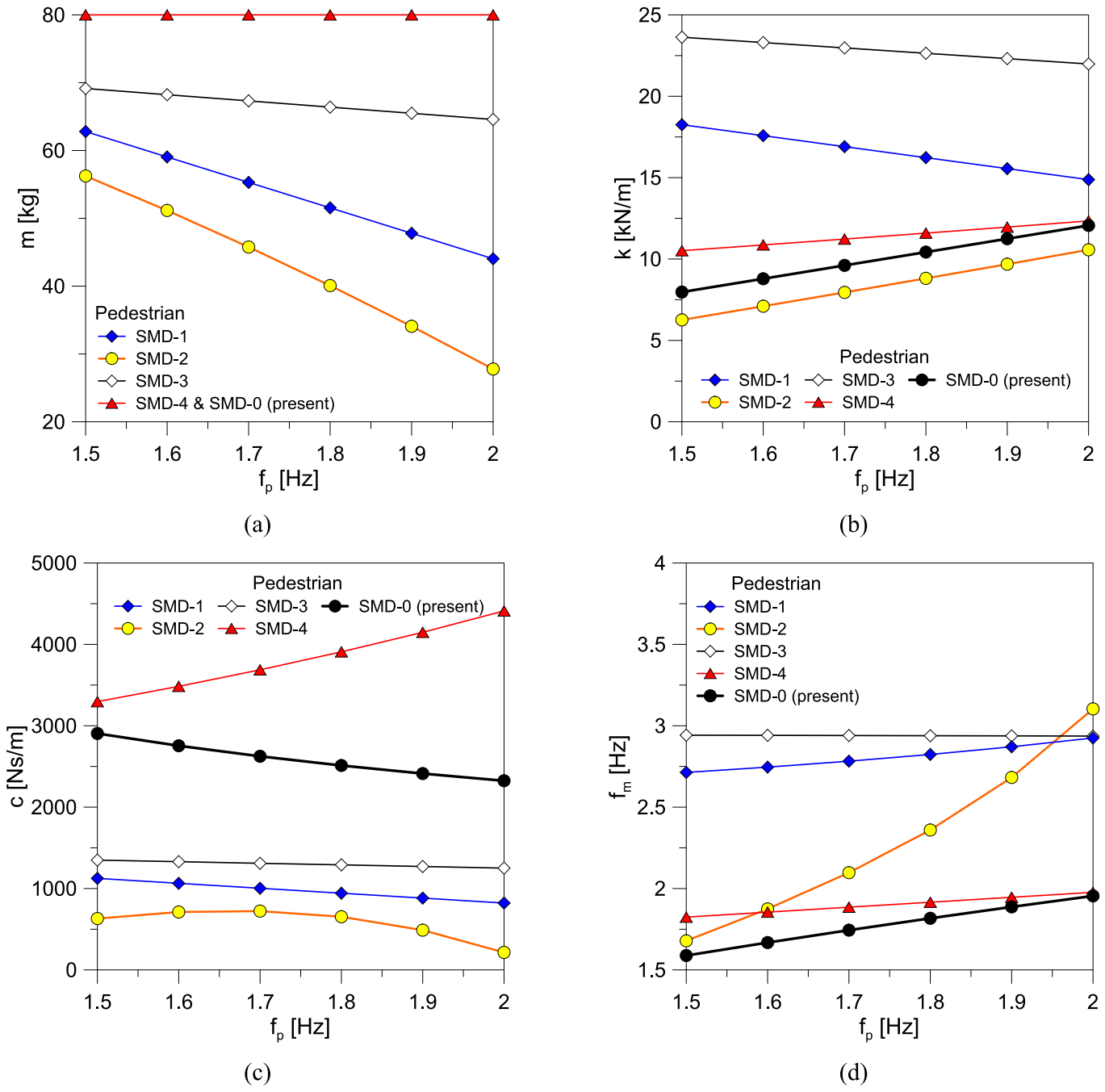

Fig. 7. Comparison of input SMD parameters, based on present calibration (SMD-0) or literature formulations (with $M = 80$ kg), in terms of (a) equivalent mass m; (b) spring stiffness k (from Eq. (19) for present model); (c) damping coefficient c (from Eq. (21) for present model); (d) undamped model frequency f_m (from Eq. (3), for present model). Analytical calculations carried out in pacing frequency range $f_p = 1.5 \div 2$ Hz (with 0.1 Hz increment).

To note that the mass of pedestrian was set in $M = 80$ kg (as for present investigations), and the corresponding parameters were analytically derived. As shown, there is a major variation in basic SMD parameters, as far as different formulations are taken into account, in terms of equivalent mass m (Fig. 7 (a)), stiffness k (Fig. 7 (b)), damping coefficient c (Fig. 7 (c)), undamped frequency f_m (Fig. 7 (d)).

Consequently, it is important to further address the effects of selected SMD approaches in terms of human-induced effects on a selection of floors.

Table 1
Summary of examined floor configurations. *= experimental frequency from [17].

Floor system	Material	Span [m]	Walking surface [m^2]	Frequency f_1 [Hz]	Mass M_s [kg]	M / M_s
F#1	Concrete	5	30	21.99	20,700	≈1/260
F#2	Concrete	5	30	11.05	10,350	≈1/130
F#3	Concrete	5	30	5.30	3,530	≈1/44
F#4	Glass	2.65	3.58	14.3 *	320	1/4

4. Parametric numerical analysis

4.1. Selected floor systems

A set of different floor systems (F#1 to F#4) was taken into account for a parametric numerical analysis inclusive of 100 dynamic simulations. Overall, the attention was focused on typical performance indicators of primary interest for vibration serviceability assessment of pedestrian structures, and thus useful to characterize the dynamic response of selected floors. In doing so, the selected floors consisted in slab configurations characterized by various vibration frequencies f_1 and structural mass M_s parameters, see Table 1.

Three concrete slabs characterized by high or low fundamental vibration frequency, and high or low mass compared to pedestrian, are taken into account for SMD assessment. At the same time, a fourth floor composed of glass and characterized by high vibration frequency but relatively small structural mass, compared to the occupant, is also investigated. The so-called F#4 system takes inspiration from earlier investigations reported in [17,23,24], where it was observed that the response of glass pedestrian systems to human-induced reactions is affected by specific intrinsic parameters. Also, basic structural components are often characterized by limited structural mass and vibration frequency which is not necessarily "low" [10]. Specific studies are thus recommended especially under unfavourable operational and ambient conditions, given that no dedicated technical regulations are available for their vibration serviceability assessment [27,28].

4.2. Structural models and performance indicators

The parametric numerical analysis was carried out in ABAQUS [29], where a set of five pedestrian models (SMD-0 to SMD-4) and four different floors (Table 1) was taken into account to explore the effects of random walks from a single occupant ($M = 80$ kg). The pacing frequency of pedestrian was explored in the range $f_p = 1.5$–2 Hz (with 0.1 Hz the increment), and a total of 100 numerical simulations were performed.

For structural modelling, the strategy schematized in Fig. 3 (a) was taken into account. To note that a conventional Rayleigh approach was taken into account to define the mass-proportional and stiffness-proportional damping terms [30]. More specifically, they were calculated as:

$$\alpha = \xi_s \frac{2\omega_1\omega_2}{\omega_1 + \omega_2} \tag{22}$$

$$\beta = \xi_s \frac{2}{\omega_1 + \omega_2} \tag{23}$$

with ω_1, ω_2 representing the natural circular frequencies for first and second vibration modes of F#1 to F#4 floors in Table 1. A conventional $\xi_s = 3\%$ damping ratio was considered for concrete slabs [2], while for glass system F#4, the latter was set in $\xi_s = 2\%$ [23].

According to several literature documents, the parametric numerical results were addressed in terms of traditional performance indicators for vibration serviceability issues of structural systems. In this manner, dynamic effects deriving from different SMD approaches were properly quantified. Human-induced accelerations on the investigated F#1 to F#4 floors were first elaborated to express the corresponding root-mean-square (RMS) value as:

$$a_{Z,RMS} = \sqrt{\frac{1}{t_n - t_{n-1}} \int_{t_{n-1}}^{t_n} a_Z^2(t)dt} \tag{24}$$

Additional quantitative comparisons were carried out in terms of peak acceleration for the examined floors ($a_{Z,peak}$), and corresponding

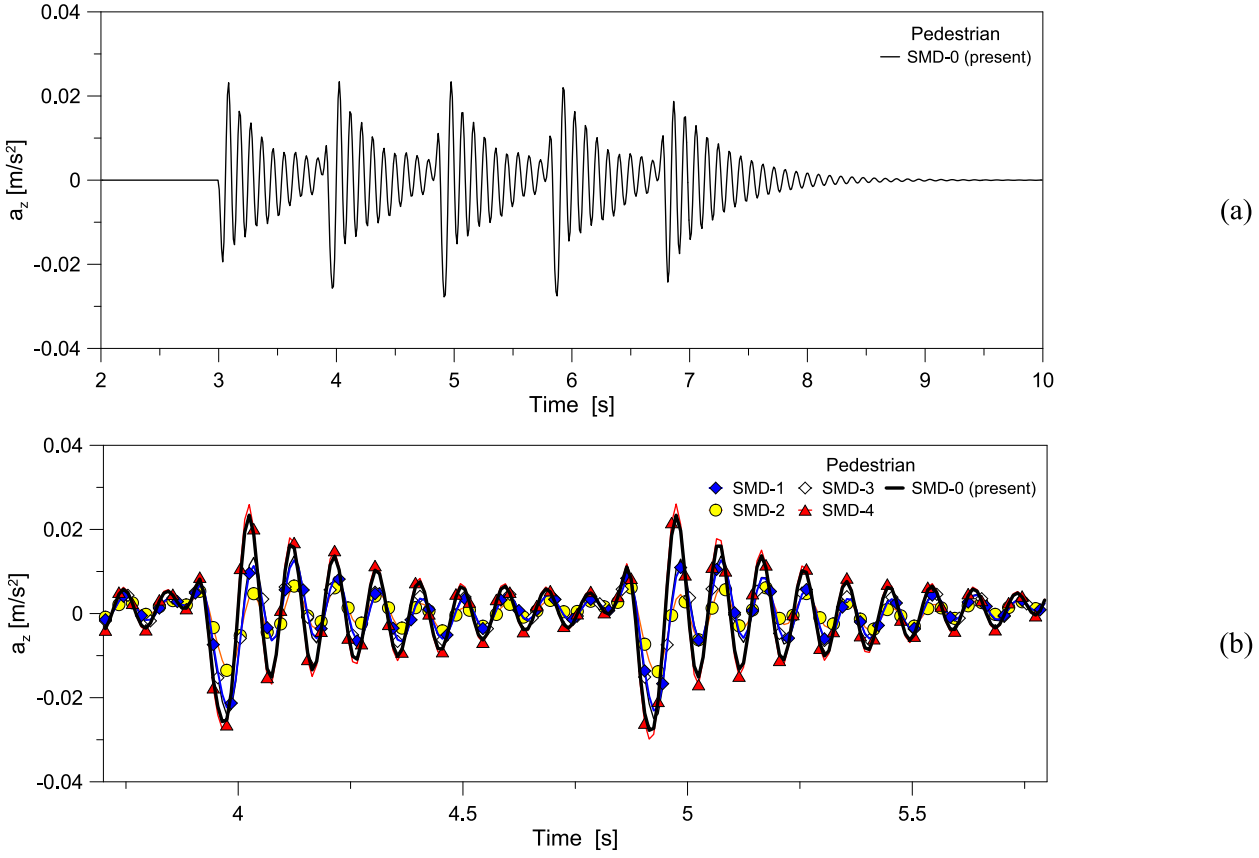

Fig. 8. Typical dynamic response of F#2 floor under human-induced vibrations (ABAQUS): (a) example of SMD-0 induced acceleration peak (with $f_p = 1.5$ Hz and $M = 80$ kg) and (b) corresponding comparison of different SMD modelling assumptions.

CREST factor:

$$CREST = \frac{a_{Z,peak}}{a_{Z,RMS}} \quad (25)$$

5. Discussion of numerical results

5.1. Floor dynamic response

The analysis of numerical results was based on vertical acceleration records at the mid-span section of each floor. The typical dynamic simulation included the preliminary application of dead (gravity) loads on each structure, and the subsequent application of human-induced loads based on SMD-0 and SMD-1 to SMD-4 approaches, for a given f_p.

Fig. 8 (a) shows the measured acceleration time history for the F#2 floor under SMD-0 modelling assumptions (with f_p = 1.5 Hz), while Fig. 8 (b) proposes a time interval selection, from the same simulation, in which the sensitivity of structural dynamic estimates based on different SMD models is further emphasized.

It is thus possible to see that (for F#2 system) the effects due to present SMD-0 proposal are rather in line with SMD-4 estimates, while acceleration peaks are progressively reduced, in the order, for SMD-3, SMD-1 and SMD-2.

5.2. Floor sensitivity to SMD strategy

In general terms, the numerical parametric investigation gave evidence of large sensitivity of selected performance indicators for the examined floor systems, as a function of the adopted SMD strategy. In this regard, the quantitative assessment of SMD-1 strategy was carried out by taking into account the total of 100 parametric analyses and the previously defined structural performance indicators. Selected examples can be seen in Figs. 9-10 in terms of RMS acceleration or acceleration peak respectively, for F#1 to F#4 slabs. At every imposed pacing frequency f_p, the corresponding performance indicator is first extracted for each SMD-*n* approach. The average result from SMD-1 to SMD-4 model is graphically emphasized (±standard deviation). The SMD-0 estimates are then compared as a function of f_p.

For all the examined configurations, it can be noted that a mean scatter up to 25–30% from the average result of SMD-1 to SMD-4 models was calculated, as a major effect of different input assumptions and higher or lower sensitivity of the F#1 to F#4 systems to human-induced vibrations. This result suggests a typically non-negligible sensitivity of floors to input SMD parameters. Besides, it is also worth to note that the SMD-0 estimates in Figs. 9-10 are generally in line with SMD-1 to SMD-4 average, and always comprised in their ± standard deviation range, both in terms of RMS acceleration and acceleration peak. This numerical

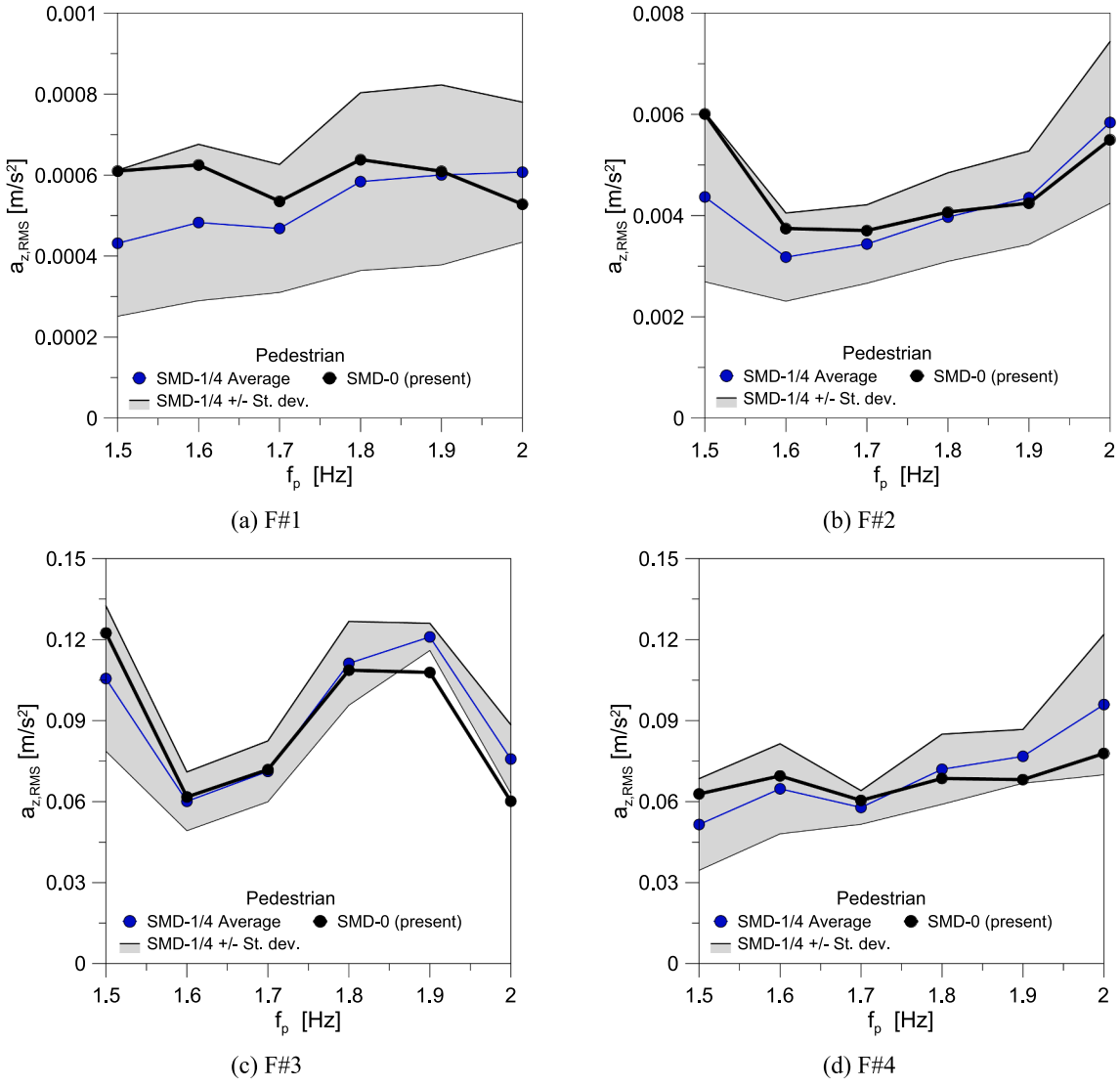

Fig. 9. Comparison of structural effects due to various SMD modelling approaches (with M = 80 kg), in terms of RMS acceleration for the examined floors (ABAQUS).

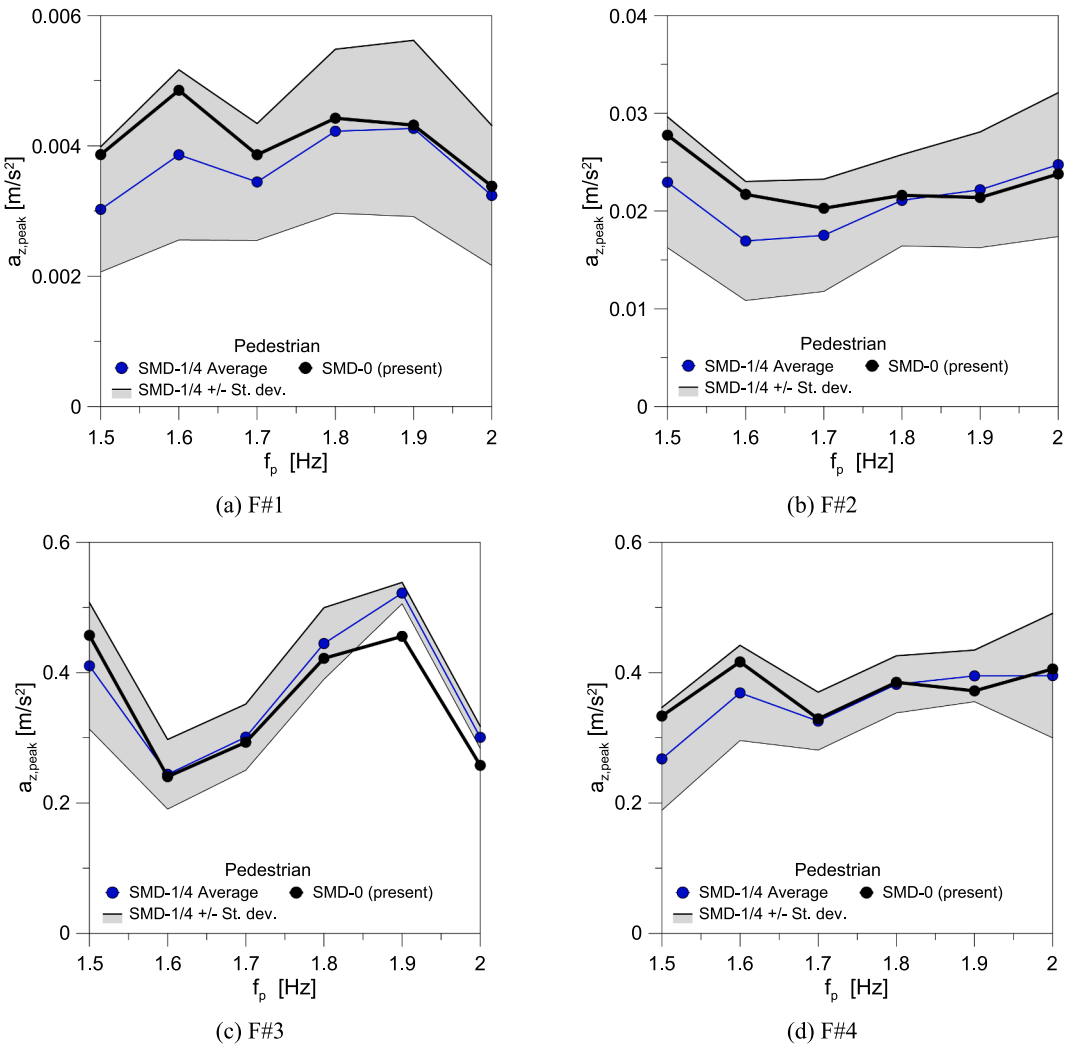

Fig. 10. Comparison of structural effects due to various SMD modelling approaches (with M = 80 kg), in terms of acceleration peak for the examined floors (ABAQUS).

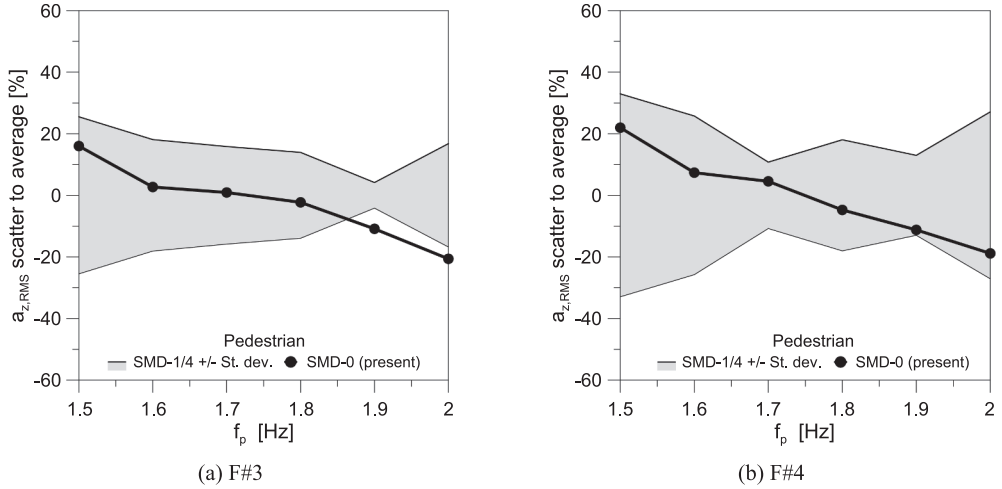

Fig. 11. Sensitivity of RMS acceleration to various SMD models (with M = 80 kg), as observed for (a) low-frequency (F#4) or (b) low-mass (F#4) floors, in terms of percentage scatter of SMD-0, towards the SMD-1 to SMD-4 average (ABAQUS).

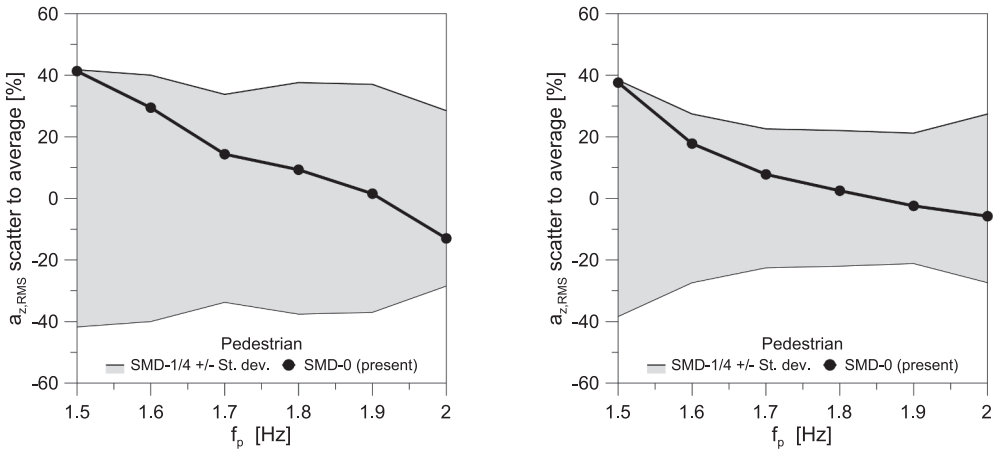

(a) F#1 (b) F#2

Fig. 12. Sensitivity of RMS acceleration to various SMD models (with $M = 80$ kg), as observed for (a)-(b) high-frequency and high-mass floors (F#1 and F#2), in terms of percentage scatter of SMD-0, towards the SMD-1 to SMD-4 average (ABAQUS).

outcome suggests a rather good potential and accuracy of SMD-0 calibration strategy for dynamic performance assessment purposes, for all the examined configurations.

5.3. Sensitivity of performance indicators

For the F#3 and F#4 floor systems, further attention was spent for the analysis of SMD effects in terms of vibration performances.

In this regard, Fig. 11 (a) and (b) show the evolution of RMS trend (as obtained from SMD-1 to SMD-4 approaches) as a function of pacing frequency f_p, in terms of percentage scatter from the calculated average $\pm$ standard deviation. As a further quantitative comparison, the SMD-0 percentage scatter from the average of SMD-1 to SMD-4 estimates is also proposed. In this regard, it is worth to note that the selected F#3 and F#4 floors are characterized by low-frequency and high-mass in the first case (F#3), and high-frequency but limited mass (compared to the occupant), in the second case (F#4), as also emphasized in Table 1. Different structural dynamics can be thus expected from F#3 and F#4 systems under human-induced vibrations.

Besides, Fig. 11 shows for both F#3 and F#4 floor a similar amplitude / trend of percentage scatter, as a function of f_p, and thus suggests similar sensitivity for them to SMD parameters.

The analysis of comparative RMS acceleration trends for the F#1 an F#2 floors (with high-frequency and high-mass properties, see Table 1) is reported in Fig. 12, and also shows a similar trend of percentage scatter for the selected SMD models. To note that the percentage values further increase compared to Fig. 11, because of the higher stiffness and mass of floors compared to SMD. As such, careful consideration should be given for the analysis of possible structural configurations of practical interest, but especially to those (like F#4, in present study) characterized by relatively low mass and relatively low-medium vibration frequency, because affected by marked sensitivity to human-induced effects.

6. Conclusions

For vibration serviceability issues in structural systems, the engineering knowledge and availability of computationally efficient and realistic modelling strategies represent a strategic task. Over the years, several formulations have been theoretically elaborated and proposed in the literature, and validated towards complex experimental investigations, in order to support a more realistic analysis of Human-Structure Interaction (HSI) phenomena in those systems (like bridges and floors) with high sensitivity to vibrations.

In this paper, the attention was focused on Spring-Mass-Damper (SMD), Single Degree of Freedom (SDOF) approaches that can be efficiently used to describe human-induced effects on structures, in terms of calibrated equivalent mass m, spring stiffness k and damping coefficient c to reproduce pedestrians.

Differing from literature approaches, the SMD parameter calibration was elaborated based on the use of a single body sensor, in the Centre of Mass (CoM) of pedestrian, which was used to track motion features and extract relevant SMD input parameters. Empirical expressions were thus formulated to predict m, k, c as a function of pacing frequency f_p, based on experimental input from up to 300 gaits. To note that the proposed SMD-0 approach can be extremely efficient when in-field measurements are required (without the support of ideal laboratory conditions) or even limited resources / sensors for testing are available.

For validation of present SMD-0 model, a set of four different floors (with high or low vibration frequency and structural mass, compared to the occupant) were taken into account to perform a parametric numerical investigation, including up to 100 dynamic simulations. The SMD-0 proposal, and its effects on structures, were thus quantitatively assessed towards a selection of four SMD formulations of literature (SMD-1 to SMD-4), in terms of typical performance indicators for structural assessment (root-mean-square (RMS) acceleration, acceleration peak, CREST factor).

The numerical parametric study proved that the present SMD-0 model, whilst optimized in number of sensors and experimental methods, can be particularly efficient for vibration serviceability purposes, and can offer rather good accuracy in terms of dynamic estimates (on the structural side), compared to other SMD approaches. Besides, it is also important to remind that the present SMD-0 validation was based (even up to 300 recorded gaits) on a single pedestrian volunteer and on a single floor setup, which suggests a further robust extension of experimental studies to a multitude of additional configurations and combinations of input parameters, on the side of pedestrians (i.e., gender, age, height, mass) and on the side of structural features (i.e., structural mass, fundamental vibration frequency, etc.). As such, additional investigations and dedicated calibrations are needed in this direction.

Declaration of Competing Interest

The authors declare that they have no known competing financial interests or personal relationships that could have appeared to influence the work reported in this paper.

Data availability

Data will be made available on request.

Acknowledgements

This research activity has been carried out at Department of Civil Engineering and Architecture of University of Trieste (Italy), and financially supported in the framework of “ComBioDyn” Microgrants 2022 project.

References

[1] H. Bachmann, W. Ammann, Vibrations in structures: Induced by man and machines, International Association for Bridge and Structural Engineering, Zurich, Switzerland, 1987.
[2] G. Sedlacek, C. Heinemeyer, C. Butz, Generalisation of Criteria for Floor Vibrations for Industrial, Office, Residential and Public Building and Gymnasium Halls; European Commission: Luxembourg, 2006.
[3] E. Shahabpoor, A. Pavic, V. Racic, Interaction between Walking Humans and Structures in Vertical Direction: A Literature Review, Shock Vib. 2016 (2016) 3430285.
[4] M. Zhang, C.T. Georgakis, J. Chen, Biomechanically excited SMD model of a walking pedestrian, J. Bridge Eng. 21 (8) (2016) C4016003.
[5] F.T. Silva, H.M.B.F. Brito, R.L. Pimentel, Modelling of crowd load in vertical direction using biodynamic model for pedestrians crossing footbridges, Can. J. Civil Eng. 40 (2013) 1196–1204.
[6] M.A. Toso, H.M. Gomes, F.T. da Silva, R.L. Pimentel, Experimentally fitted biodynamic models for pedestrian-structure interaction in walking situations, Mech. Syst. Signal Process. 72–73 (2016) 590–606.
[7] M.S. Pfeil, W.D. Varela, N. de Paula Amador da Costa, Experimental calibration of a one degree of freedom biodynamic model to simulate human walking-structure interaction, Eng. Struct. 262 (2022).
[8] H. Wang, J. Chen, J.M.W. Brownjohn, Parameter identification of pedestrian’s spring-mass-damper model by ground reaction force records through a particle filter approach, J. Sound Vibration 411 (2017) 409–421.
[9] C. Bedon, Body CoM Acceleration for Rapid Analysis of Gait Variability and Pedestrian Effects on Structures, Buildings 12 (2) (2022) 251, https://doi.org/10.3390/buildings12020251.
[10] C. Bedon, M. Fasan, S. Noè, Body Motion Sensor Analysis of Human-Induced Dynamic Load Factor (DLF) for Normal Walks on Slender Transparent Floors, J. Sens. Actuator Netw. 11 (2022) 81, https://doi.org/10.3390/jsan11040081.
[11] S. Živanovic, A. Pavic, P. Reynolds, Vibration serviceability of footbridges under human-induced excitation: A literature review, J. Sound Vib. 279 (2005) 1–74.
[12] B. Ellingwood, A. Tallin, Structural serviceability: Floor vibrations, J. Struct. Eng. (1984) 401–418, https://doi.org/10.1061/(ASCE)0733-9445(1984)110:2(401).
[13] R. Sachse, A. Pavic, P. Reynolds, Human-structure dynamic interaction in civil engineering dynamics: A literature review, Shock Vib. Digest 35 (2003) 3–18.
[14] F. Alami, M. Helmi, V.A. Noorhidana, Fiber reinforced polymer as potential solution for vibration problem in concrete slab for supporting human comfortable, IOP Conf. Ser.: Earth Environ. Sci. 739 (2021), 012025, https://doi.org/10.1088/1755-1315/739/1/012025.
[15] P. Junges, H.L.L. Rovere, R.C.d.A. Pinto, Vibration Analysis of a Composite Concrete/GFRP Slab Induced by Human Activities, J. Compos. Sci. 1 (2017) 11, https://doi.org/10.3390/jcs1020011.
[16] C. Bedon, Experimental investigation on vibration sensitivity of an indoor glass footbridge to walking conditions, J. Build. Eng. 29 (2020), 101195.
[17] C. Bedon, Diagnostic analysis and dynamic identification of a glass suspension footbridge via on-site vibration experiments and FE numerical modelling, Compos. Struct. 216 (2019) 366–378.
[18] P.G. Adamczyk, A.D. Kuo, Redirection of center-of-mass velocity during the step-to-step transition of human walking, J. Exp. Biol. 212 (2009) 2668–2678.
[19] M. Bocian, J.H.G. Macdonald, J.F. Burn, Biomechanically inspired modeling of pedestrian-induced vertical self-excited forces, J. Bridge Eng. (2013) 1336–1346, https://doi.org/10.1061/(ASCE)BE.1943-5592.0000490.
[20] B. Koopman, H.J. Grootenboer, H.J. de Jongh, An inverse dynamics model for the analysis, reconstruction and prediction of bipedal walking, J. Biomech. 28 (1995) 1369–1377.
[21] H. Geyer, A. Seyfarth, R. Blickhan, Compliant leg behaviour explains basic dynamics of walking and running, Proceedings of the Royal Society Biological Sciences 273 (2006) 2861–2867.
[22] Q.S. Yang, J.W. Qin, S.S. Law, A three-dimensional human walking model, J. Sound Vibration 357 (2015) 437–456.
[23] C. Bedon, S. Noè, Post-Breakage Vibration Frequency Analysis of In-Service Pedestrian Laminated Glass Modular Units, Vibration 4 (2021) 836–852.
[24] C. Bedon, S. Noè, Uncoupled Wi-Fi Body CoM Acceleration for the Analysis of Lightweight Glass Slabs under Random Walks, Journal of Sensor and Actuator Networks 11 (1) (2022) 10.
[25] MATLAB (R2018a); Version 9.4 Natick; The MathWorks Inc.: Natick, MA, USA, 2018.
[26] Bertos, G.; Childress, D.; Gard, S. The vertical mechanical impedance of the locomotor system during human walking with applications in rehabilitation, in: Proceeding of the 2005 IEEE Ninth International Conference on Rehabilitation Robotics, 2005, Chicago.
[27] CEN/TC 250; prCEN/TS xxxx-1: 2019—In-Plane Loaded Glass Components. CEN—European Committee for Standardization: Brussels, Belgium, 2019.
[28] CEN/TC 250; prCEN/TS xxxx-2: 2019—Out of-Plane Loaded Glass Components. CEN—European Committee for Standardization: Brussels, Belgium, 2019.
[29] ABAQUS Computer Software v.6.14; Simulia: Dassault, RI, USA, 2021.
[30] R.W. Clough, J. Penzien, Dynamics of Structures; McGrawHill: Berkeley, CA, USA, 1993.